Memo 95

Antenna Noise Temperature Calculation

Germán Cortés Medellín

07/07

US-SKA Technical Memo Series

Antenna Noise Temperature Calculation

Germán Cortés Medellín
National Astronomy and Atmospheric Center, Cornell University
Ithaca, NY, September 22, 2004

1 Introduction

This antenna technical memo is intended to serve as a guideline for the calculation of the antenna noise temperature of a single antenna element[1] including noise contribution from atmospheric, ground and cosmic sources.

We define the system input noise temperature or *system temperature* (for short) by,

$$T_{SYS} \quad = \quad \eta_L \, T_A + (1 - \eta_L) \, T_p + T_{REC} \tag{1}$$

where, T_A is the *antenna noise temperature* (See Equation 2 below), η_L is the *antenna radiation efficiency*, T_p is the physical temperature of the antenna, and T_{REC} is the *receiver noise temperature* including possible mismatches.

2 Antenna Noise Temperature

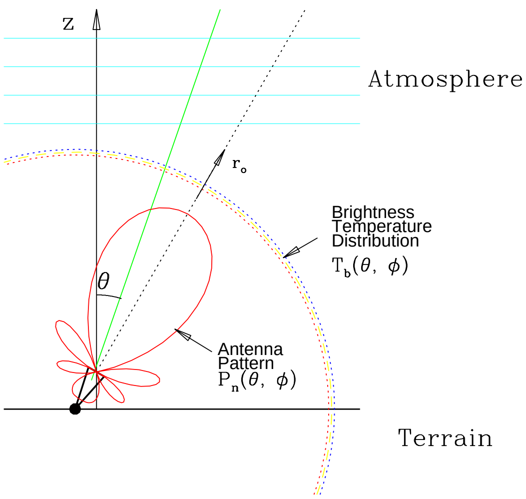

Figure 1: Relation between antenna temperature, antenna radiation pattern and the brightness temperature of the observed scene.

Let's consider a lossless antenna pointing in the direction $\hat{\mathbf{r}}_o$, as shown in Figure 1, then, the radiometric noise temperature, for a single mode at the i^{th} port, at a given frequency ν, is given by [Ulaby, 1981]:

$$T_A(\nu \,|\hat{\mathbf{r}}_o) \quad = \quad \frac{\displaystyle\iint_{4\pi} T_b(\nu, \theta, \phi) \, P_n(\nu, \theta, \phi \,|\hat{\mathbf{r}}_o) \, \sin\theta \, d\theta \, d\phi}{\displaystyle\iint_{4\pi} P_n(\nu, \theta, \phi) \, \sin\theta \, d\theta \, d\phi} \tag{2}$$

[1]For an array such as the SKA where the antenna elements extend across hundreds or thousands of kilometers, local variations in atmospheric and ground emissions may have to be taken into account when calculating the array noise temperature in the same way as is the case for VLBI.

where, $P_n(\nu, \theta, \phi\,|\hat{\mathbf{r}}_o)$ is the *total* (Co-polar + Cross-polar) radiation antenna pattern for that particular polarization port when the antenna is pointing in the direction $\hat{\mathbf{r}}_o$. $T_b(\nu, \theta, \phi)$ is the *apparent radiometric temperature distribution*, also known as the *brightness temperature distribution*, from the "scene" surrounding the antenna (see Figure 1), at that particular frequency.

There are different source contributions to the brightness temperature distribution surrounding the antenna, one is the emission from the gases in the atmosphere, the second is the apparent temperature of the background sky seen through the atmosphere and other is the emission and scattering from the ground. We are going to go in more detail over each one of these in the following sections.

3 Brightness Temperature

3.1 Brightness Temperature and Radiative Transfer

Radiative transfer theory describes the intensity of radiation propagating in a media, such as the atmosphere, that absorb, emit and scatter radiation. The radiation field is described in terms of the *specific intensity*, I_ν, [W m^{-2} str^{-1} Hz^{-1}], which is the power per unit area, per unit frequency interval at a specific frequency, and per unit solid angle, flowing in a given direction.
In the atmosphere, radiation emitted by molecules is in part attenuated by atmospheric absorption; the energy absorbed is re-emitted as thermal radiation. The amount of attenuation depends on the distance travel by the radiation through the medium. Then, the specific intensity received from a given direction in the atmosphere[2] is given by, [Janssen, 1993].

$$I_\nu \;=\; I_\nu(s_o)\, e^{-\tau_\nu(0,s_o)} + \int_0^{s_o} \kappa_a(\nu, s)\, B_\nu(T)\, e^{-\tau_\nu(0,s)}\, ds, \tag{3}$$

where $I_\nu(s_o)$ is the background intensity at a distance s_o, $\kappa_a(\nu, s)$ is the *atmospheric absorption coefficient*, $B_\nu(T)$, is the source within the medium, which in the case of an isothermal medium, corresponds to the Planck's function:

$$B_\nu(T) \;=\; \frac{2h\nu^3}{c^2}\, \frac{1}{e^{h\nu/kT} - 1}, \tag{4}$$

h is Planck's constant, k is Boltzmann's constant, ν is the frequency, and c is the speed of light. Finally, τ_ν is the *optical depth* or *opacity* of the medium, defined by,

$$\tau_\nu(s_o, s) \;=\; \int_{s_o}^{s} \kappa_a(\nu, \xi)\, d\xi. \tag{5}$$

At microwave frequencies, with $h\nu << kT$, the Planck's function can be approximated by,

$$B_\nu(T) \;\approx\; \frac{2kT}{\lambda^2}, \tag{6}$$

this is called the Rayleigh-Jeans approximation. The linear dependence of the Planck's function (specific intensity) on the physical temperature allows to define the *brightness temperature*, T_b,

$$T_b \;=\; \frac{\lambda^2}{2k}\, I_\nu. \tag{7}$$

Then, Equation 3 can be rewritten as,

$$T_b(\nu) \;=\; T_{bo}(\nu)\, e^{-\tau_\nu(0,s_o)} + \int_0^{s_o} \kappa_a(\nu, s)\, T(s)\, e^{-\tau_\nu(0,s)}\, ds. \tag{8}$$

where $T_{bo}(\nu)$ is the background brightness temperature, which in our case, when looking through the atmosphere, is due to cosmic emission.

[2] Ignoring scattering contributions in the atmosphere

3.2 Atmospheric Absorption Coefficient

The absorption coefficient is a macroscopic parameter that represents the interaction of incident electro-magnetic radiation with the constituent molecules of the atmosphere. It is a function of the energy $(h\nu)$ of the incident radiation field, the transition probability between two molecular states, and the energy difference between these two states, $(E_a - E_b)$. The state of the molecule is represented by a wave function ψ that obeys the Schrödinger equation, [Merzbacher, 1970],

$$\mathcal{H}\psi = E\psi \tag{9}$$

where, $\mathcal{H}$ is the Hamiltonian operator and E the energy of the state. ψ depends on the coordinates of all particles. In simple molecules such as those that constitute the atmosphere, ψ can be separated into several components: an electronic part, a vibrational part, a rotational part, and a nuclear spin, i.e.,

$$\psi = \psi_{elec}\, \psi_{vib}\, \psi_{rot}\, \psi_{nuc}. \tag{10}$$

Transitions between electronic states occur in the ultraviolet, vibrational transitions occur in the infrared and rotational transitions occur in the microwave, millimeter, sub-millimeter and long infrared frequencies. The energy associated with the nuclear spin produces transitions in the MHz range.

In order to characterize the transitions between states of a given molecular species, at a frequency ν, we define the power-*absorption coefficient* [Rosenkranz, 1993],

$$\kappa_\nu = n \sum_{i,j} S_{ij}(T)\, F(\nu, \nu_{ij}), \tag{11}$$

where n is the number of molecules of the given species per unit volume, f and i denote the energy state of an isolated molecule, $S_{ij}(T)$ is the line intensity at temperature T of a single line for a single molecule, $F(\nu, \nu_{ij})$ is the line-shape function, and $\nu_{ij} = (E_f - E_i)/h$, is the frequency of the absorbed (or emitted) photon when the molecule passes form the initial to the final state.

Transitions of interest at microwave frequencies that occur in the atmosphere are rotational transitions in the ground vibrational state of molecules, and account for the microwave spectra of H_2O, O_3, CO and N_2O.

For an isolated, stationary molecule, $F(\nu, \nu_{ij}) \to \delta(\nu, \nu_{ij})$; in reality, the molecules are in constant motion, interacting and colliding with one another. These disturbances cause the spectral lines to spread in frequency about the line center frequency ν_{if}, this is called *line-broadening.* There are two important line-broadening mechanisms in the atmosphere: Doppler (or thermal), and collisional (or pressure) line broadening.

For atmospheric pressures ranging from 1 to 1000 mbar, collisions between molecules are the dominant line broadening mechanism. Collisional broadening is approximated by the Lorentzian line shape,

$$F_c(\nu, \nu_{ij}) = \frac{1}{\pi} \left(\frac{\nu}{\nu_{ij}}\right)^2 \frac{\Delta\nu_c}{(\nu - \nu_{ij})^2 + \Delta\nu_c^2}. \tag{12}$$

$\Delta\nu_c$, the collisional half-width of the line, is function of the atmospheric pressure P and inversely proportional to the atmospheric temperature T,

$$\Delta\nu_c = \gamma_{co}\, (P/P_o)\, (T_o/T)^x, \tag{13}$$

where $x \approx 0.75$.

Microwave ground based observations of atmospheric species are limited by atmospheric absorption due mainly to tropospheric water vapor and oxygen. There are two main effects of atmospheric absorption spectra of O_2 and H_2O. First, troposphere high pressure broadens the spectral lines so the influence of atmospheric transitions of O_2 and H_2O spans several GHz at the wings of the lines. Second, water vapor column is the dominant source of attenuation of ground based observations.

Therefore, for antenna noise temperature calculations in the frequency range for SKA, we could reduce the atmospheric absorption coefficient to:

$$\kappa_a(\nu, z) = \kappa_{H_2O}(\nu, z) + \kappa_{O_2}(\nu, z) \quad (14)$$

where we have included the dependence on pressure and temperature implicitly in the position z of the molecule species in the atmosphere.

3.3 Atmospheric Absorption Models

There are several models available for the calculation of atmospheric absorption and attenuation. The astronomy community uses mainly: atmospheric transmission (AT) [Grossman, 1989]; atmospheric transmission at microwaves (ATM) [Pardo et al. 2001] and several codes based on Liebe's microwave propagation model (MPM) [Liebe, 1989]. There are also several radiative transfer codes based on well-known line databases like HITRAN [Rothman et al., 1992] and JPL [Pickett et al., 1998].

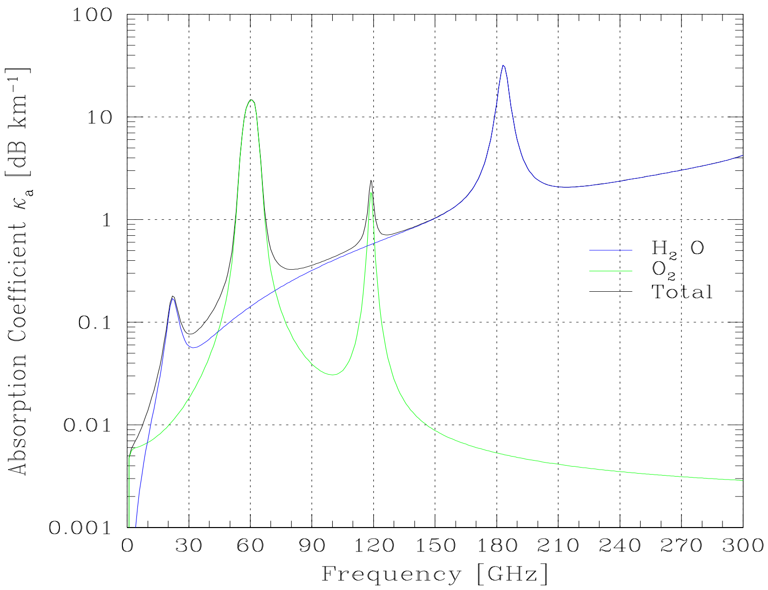

Figure 2: Microwave absorption due water vapor and oxygen in the atmosphere. Surface conditions: $P = 1013$ mbar, $T = 293$ K, and water column of $\rho = 7.5$ g cm^{-3}.

In the interest of being self-contained we are including here two simple models following [Ulaby, 1981] (ch. 5), which in turn are based on [Waters, 1976], and [Rosenkranz, 1975], to calculate the absorption coefficients of water vapor and molecular oxygen in the atmosphere for microwave and millimeter-wave frequencies.

Figure 2 shows the calculated atmospheric attenuation as a function of frequency from 0 to 300 GHz, at sea level conditions, following this formulation. The O_2 absorption spectrum consists of a single line at 118.75 GHz, and a large number of absorption lines spanning from 50 to 70 GHz, that atmospheric pressure blend into a continuous absorption band centered around 60 GHz. H_2O, has very important absorption lines at 22.235 and 183.31 GHz.

3.3.1 Water-Vapor Absorption

The absorption coefficient for the water vapor in the atmosphere can be approximated by [Ulaby, 1981]:

$$\kappa_{H_2O}(\nu) = 2\,\nu^2\,\rho_v\left(\frac{300}{T}\right)^{5/2}\sum_{i=1}^{i_{max}} A_i\,e^{-\mathcal{E}_i'/T}\,\mathcal{F}_{H_2O}(\nu,\nu_i) + \Delta\kappa(\nu) \qquad \text{[dB/km]} \quad (15)$$

with, the line shape given by,

$$\mathcal{F}_{H_2O}(\nu,\nu_i) = \frac{\gamma_i}{(\nu_i^2-\nu^2)^2+4\,\nu^2\,\gamma_i^2} \tag{16}$$

$$\gamma_i = \gamma_{i0}\left(\frac{P}{1013}\right)\left(\frac{300}{T}\right)^{x_i}\left[1+10^{-2}\,a_i\,\frac{\rho_v\,T}{P}\right] \qquad \text{[GHz]} \tag{17}$$

where, ρ_v is the water vapor density in the atmosphere in g/m^3, P is the atmospheric pressure in $mbars$, and T is the atmospheric temperature in K, and ν the frequency in GHz. Equation 15 also includes an empirically derived correction term to the absorption coefficient, $\Delta\kappa$, of the following form:

$$\Delta\kappa(\nu) = 4.69\times10^{-6}\,\rho_v\left(\frac{P}{1000}\right)\left(\frac{300}{T}\right)^{2.1}\nu^2 \qquad \text{[dB/km]} \tag{18}$$

Values for the first 10 transition line parameters are presented in Table 1

Table 1: Water vapor line absorption transition parameters [Ulaby, 1981]

i	ν_i [GHz]	$\mathcal{E}_i'$ $[K^{-1}]$	A_i	γ_{i0} [GHz]	a_i	x_i
1	22.23515	644	1.0	2.85	1.75	0.626
2	183.31012	196	41.9	2.68	2.03	0.649
3	323.	1850	334.4	2.30	1.95	0.420
4	325.1538	454	115.7	3.03	1.85	0.619
5	380.1968	306	651.8	3.19	1.82	0.630
6	390.	2199	127.0	2.11	2.03	0.330
7	436.	1507	191.4	1.50	1.97	0.290
8	438.	1070	697.6	1.94	2.01	0.360
9	442.	1507	590.2	1.51	2.02	0.332
10	448.0008	412	973.1	2.47	2.19	0.510

3.3.2 Oxygen Absorption

The oxygen absorption coefficient for a concentration of 0.21 by volume in the air is given by [Rosenkranz, 1975],

$$\kappa_{O_2}(\nu) = 1.61\times10^{-2}\,\nu^2\left(\frac{P}{1013}\right)\left(\frac{300}{T}\right)^2\mathcal{F}_{O_2}(\nu,\nu_{if}) \qquad \text{[dB/km]} \tag{19}$$

where, ν is the frequency (GHz), P is the atmospheric pressure ($mbars$), and T is the atmospheric temperature (K). The line shape has two components: a resonant and non-resonant parts,

$$\mathcal{F}_{O_2}(\nu,\nu_{if}) = \frac{0.7\,\gamma_b}{\nu^2+\gamma_b^2}+\sum_{j=1,j\ odd}^{J_{max}}\Phi_j\left[g_{j^+}(\nu)+g_{j^+}(-\nu)+g_{j^-}(\nu)+g_{j^-}(-\nu)\right] \tag{20}$$

with,

$$\Phi_j = 4.6\times10^{-3}\left(\frac{300}{T}\right)(2j+1)\,e^{-6.89\times10^{-3}\left(\frac{300}{T}\right)j\,(j+1)} \tag{21}$$

$$g_{j^\pm}(\nu) = \frac{\gamma_j\,d_{j\pm}^2+P\,(\nu-\nu_{j\pm})\,Y_{j\pm}}{(\nu-\nu_{j\pm})^2+\gamma_j^2} \tag{22}$$

where, Φ_j is the fractional population of the initial state associated with the line. γ_j and γ_b are the *resonant* and *non-resonant* line-width parameters given by,

$$\gamma_j = 1.18 \left(\frac{P}{1013}\right)\left(\frac{300}{T}\right)^{0.85} \qquad \gamma_b = 0.49 \left(\frac{P}{1013}\right)\left(\frac{300}{T}\right)^{0.89} \tag{23}$$

And, the amplitude of the $\nu_j^{\pm}$ lines, $d_{j^{\pm}}$, is given by,

$$d_{j^+} = \left[\frac{j\,(2\,j+3)}{(j+1)(2\,j+1)}\right]^{1/2}, \qquad d_{j^-} = \left[\frac{(j+1)(2\,j-1)}{j\,(2\,j+1)}\right]^{1/2} \tag{24}$$

Table 2 gives the value of the first 20 line absorption parameters for atmospheric O_2 from [Rosenkranz, 1975], including the *interference coefficients* $Y_{j^{\pm}}$.

Table 2: First twenty O_2 line absorption parameters [Rosenkranz, 1975]

j	Resonant ν_j^+ [GHz]	Frequencies ν_j^- [GHz]	Interference Y_j^+ [mbar^{-1}]	Coefficients Y_j^- [mbar^{-1}]
1	56.2648	118.7503	4.51×10^{-4}	-2.14×10^{-5}
3	58.4466	62.4863	4.94×10^{-4}	-3.78×10^{-4}
5	59.5920	60.3061	3.52×10^{-4}	-3.92×10^{-4}
7	60.4348	59.1642	1.86×10^{-4}	-2.68×10^{-4}
9	61.1506	58.3239	3.30×10^{-5}	-1.13×10^{-4}
11	61.8002	57.6125	-1.03×10^{-4}	3.44×10^{-5}
13	62.4112	56.9682	-2.23×10^{-4}	1.65×10^{-4}
15	62.9980	56.3634	-3.32×10^{-4}	2.84×10^{-4}
17	63.5685	55.7838	-4.32×10^{-4}	3.91×10^{-4}
19	64.1278	55.2214	-5.26×10^{-4}	4.93×10^{-4}
21	64.6789	54.6711	-6.13×10^{-4}	5.84×10^{-4}
23	65.2241	54.1300	-6.99×10^{-4}	6.76×10^{-4}
25	65.7647	53.5957	-7.74×10^{-4}	7.55×10^{-4}
27	66.3020	53.0668	-8.61×10^{-4}	8.47×10^{-4}
29	66.8367	52.5422	-9.11×10^{-4}	9.01×10^{-4}
31	67.3694	52.0212	-1.03×10^{-3}	1.03×10^{-3}
33	67.9007	51.5030	-9.87×10^{-4}	9.86×10^{-4}
35	68.4308	50.9873	-1.32×10^{-3}	1.33×10^{-3}
37	68.9601	50.4736	-7.07×10^{-4}	7.01×10^{-4}
39	69.4887	49.9618	-2.58×10^{-3}	2.64×10^{-3}

3.4 Cosmic Emission

The background cosmic emission term, $T_{bo}(\nu)$, in Equation 8 may be reduced for practical purposes to two components:

$$T_{bo}(\nu) = T_{CMB} + T_{gal}(\nu) \tag{25}$$

With $T_{CMB} = 2.73K$, is the *cosmic microwave background* emission and $T_{gal}(\nu)$ is the *galactic* emission (mostly synchrotron emission), which follows a power spectrum law:

$$T_{gal}(\nu) \;=\; T_{g_o}\left(\frac{\nu_o}{\nu}\right)^{\beta} \tag{26}$$

Here we have to make the following observations: first, both, the base temperature T_{g_o} and the *spectral index* β, are functions of the observed direction in the sky. For example [Giardino et al. 2002], at 408 MHz, T_{g_o} varies from a minimum of $3K$ to maximum of $507K$, the latter in the direction of the galactic center, and with a value of $18K$ at the galactic poles. At the same time, β varies from 2.5 at in the direction of the galactic center to 3.2 within a small region just above the galactic plane. Second, the average value of β is a slow varying function of frequency, i.e., between 0.408 and 2.326 GHz is $\langle\beta_{0.408/2.326}\rangle = 2.75 \pm 0.12$, meanwhile, between 0.408 and 30 GHz is $\langle\beta_{0.408/30}\rangle = 2.91 \pm 0.09$. And third, the brightness temperature also depends on the angular size resolution, i.e., for angular resolutions of less than 55 arc min, the brightness temperature in the direction of the galactic center is reportedly $> 1,200K$ at 408 MHz [Haslam et al., 1982] and [Lawson et al., 1987].

By adopting an average value of $\beta = 2.75$, with $T_{g_o} = 20K$ at $\nu_o = 0.408$ GHz, it is possible to obtain very reasonable results for galactic contributions to the antenna noise calculations for frequencies $\nu \geq 0.01$ GHz.

3.5 Simplified Models for Ground-Based Observations

Ground-based observations usually assume a simplified model of a plane horizontally stratified atmosphere, as shown in Figure 1, with θ is the observation angle with respect to the zenith. Using Equation 8 with this approximation, we obtain that the sky brightness temperature measured from the ground is given by,

$$T_b^{sky}(\nu,\theta) \;=\; T_{bo}(\nu)\, e^{-\tau_\nu(0,\infty)\,\sec\theta} + \sec\theta \int_0^\infty \kappa_a(\nu,\zeta)\, T(\zeta)\, e^{-\tau_\nu(0,\zeta)\,\sec\theta}\, d\,\zeta, \tag{27}$$

where $T_{bo}(\nu)$ is the background brightness temperature due to cosmic emission (Equation 25), and,

$$\tau_\nu(0,\infty) \;=\; \int_0^\infty \kappa_a(\nu,\zeta)\, d\,\zeta \tag{28}$$

is the *zenith opacity*[3].

This approximation is valid for zenith angles $\theta \leq 75^o$; for angles $> 75^o$ corrections may be included to account for the finite curvature of the Earth, see for example [Han & Westwater, 2000].

3.5.1 Atmospheric Profiles

Since $\kappa_a(\nu, z)$ is function of temperature $T(z)$, pressure $P(z)$ and air density $\rho(z)$, therefore, profiles of these variables as a function of height need to be included when calculating the opacity. Atmospheric profiles for these variables based on the 1962 U.S. Standard Atmosphere are given below.

Temperature Profile

$$T(z) \;=\; \begin{cases} 288.15 + 6.5\,z & 0 \leq z \leq 11\,\text{km} \\ T(11) & 11 \leq z \leq 20\,\text{km} \\ T(11) + (z - 20) & 20 \leq z \leq 32\,\text{km} \end{cases} \tag{29}$$

where $T(z)$ is in K.

Density Profile

$$\rho_{air} \;=\; 1.225\, e^{-z/H_a}\,[1 + 0.3\,\sin(z/H_a]\qquad \text{kg m}^{-3} \tag{30}$$

[3] κ_a given here is in dB km^{-1} and it should be expressed in NP km^{-1} to be used in the calculations, i.e., $\kappa_a[\text{NP/km}] = 0.23\kappa_a[\text{dB/km}]$

where the *density scale height* $H_a = 7.3$ km.

Pressure Profile

$$P(z) \quad = \quad 1013.25\, e^{-z/H_p} \qquad \text{mbar} \tag{31}$$

where the *pressure scale height* $H_p = 7.7$ km.

Water Vapor Profile

$$\rho_v(z) \quad = \quad 7.72\, e^{-z/H_v} \qquad \text{g m}^{-3} \tag{32}$$

where the *water vapor scale height* $H_v = 2$ km.

Figure 3 shows and example of the calculated sky brightness as a function of frequency for different zenith angles.

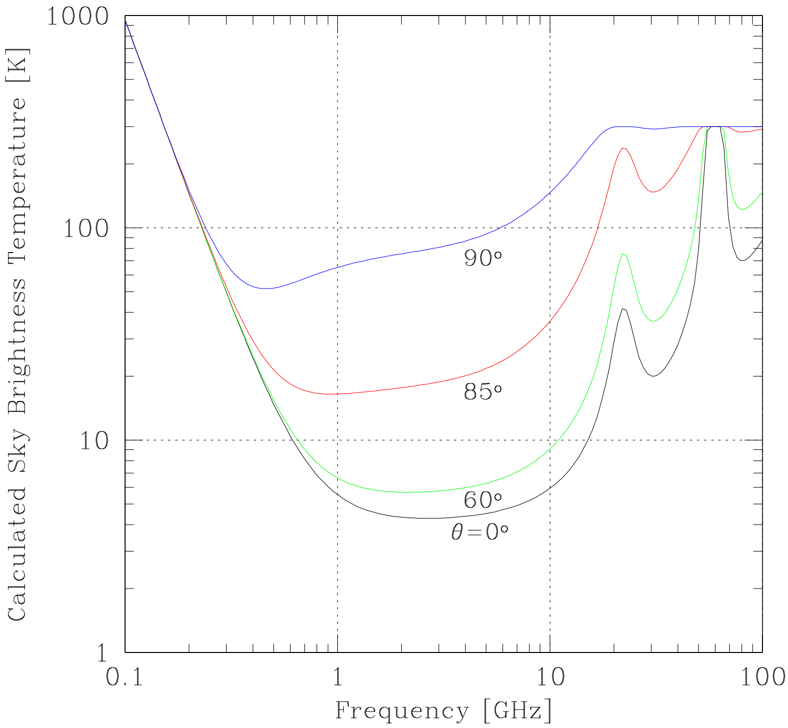

Figure 3: Calculated Sky Brightness Temperature as a function of frequency including the cosmic background radiation of 2.7 K and the galactic emission away from the plane of the galaxy, for different zenith angles.

4 Ground Emission and Background Scattering

It is important to notice that the antenna noise temperature T_A defined by Equation 2 is for a single medium. When we want to include emission and scattering from the ground, we need to modify the integrand, i.e., $T_b\, P_n$, since ground emission and scattering is a polarization dependent process. Therefore, we write:

$$T_b(\ldots)\, P_n(\ldots) \quad = \quad \begin{cases} T_b^{sky}\, P_n & 0 \leq \theta < \pi/2 \\ T_{b\,\parallel}\, P_\parallel + T_{b\,\perp}\, P_\perp & \pi/2 \leq \theta \leq \pi \end{cases} \tag{33}$$

4.1 Obtaining $P_{||}$ and $P_{\perp}$

In order to expressP_n in terms of $P_{||}$ and $P_{\perp}$, let's consider E_1,and E_2 as the *single mode* fields coming out of port-1 and port-2 of a *receiving* antenna due to a field distribution $\mathbf{E}_a$ in the far field. Henceforth, we can write,

$$E_i \;=\; S_{ip}\, E_{ap} + S_{iq}\, E_{a_q} \tag{34}$$

with, $i = \{1, 2\}$, and S_{ip} and S_{iq} are respectively the Co-Polar and Cross-Polar *receiving far field distribution*[4] of the antenna, and,

$$E_{a_p} \;=\; \hat{\epsilon}_p \cdot \mathbf{E}_a \qquad\qquad E_{a_q} \;=\; \hat{\epsilon}_q \cdot \mathbf{E}_a \tag{35}$$

where, $\hat{\epsilon}_p$ and $\hat{\epsilon}_q$ are the co-polar and cross-polar (complex) unit vectors, respectively.

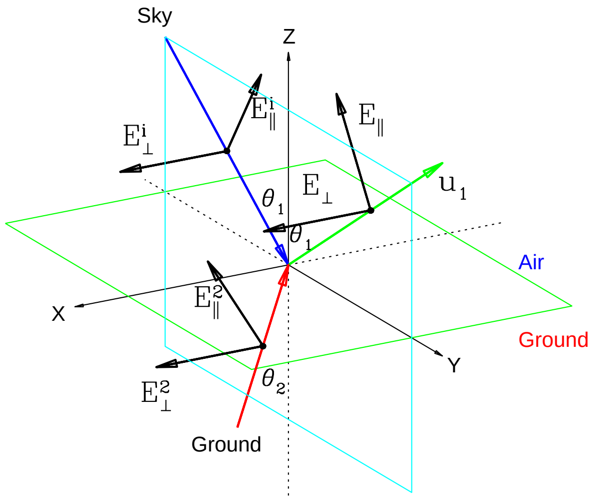

Figure 4: Geometry of the ground emission and sky background scattering of termal noise.

In order to include noise emission and scattering from the ground, we need to to express $\mathbf{E}_a$ in terms of $\hat{\mathbf{u}}_{||}$ and $\hat{\mathbf{u}}_{\perp}$ directions to the plane of incidence at the surface interaction (see Figure 4), i.e.,

$$\mathbf{E}_a \;=\; \mathcal{E}_{||}\, \hat{\mathbf{u}}_{||} + \mathcal{E}_{\perp}\, \hat{\mathbf{u}}_{\perp} \tag{36}$$

Therefore,

$$E_{a_p} \;=\; \hat{\epsilon}_p \cdot \mathbf{E}_a \;=\; \mathcal{E}_{||}\, \left(\hat{\epsilon}_p \cdot \hat{\mathbf{u}}_{||}\right) + \mathcal{E}_{\perp}\, \left(\hat{\epsilon}_p \cdot \hat{\mathbf{u}}_{\perp}\right) \tag{37}$$

$$E_{a_q} \;=\; \hat{\epsilon}_q \cdot \mathbf{E}_a \;=\; \mathcal{E}_{||}\, \left(\hat{\epsilon}_q \cdot \hat{\mathbf{u}}_{||}\right) + \mathcal{E}_{\perp}\, \left(\hat{\epsilon}_q \cdot \hat{\mathbf{u}}_{\perp}\right) \tag{38}$$

Then, at port 1,

$$E_1 \;=\; S_{1p}\, \left[\mathcal{E}_{||}\, \left(\hat{\epsilon}_p \cdot \hat{\mathbf{u}}_{||}\right) + \mathcal{E}_{\perp}\, \left(\hat{\epsilon}_p \cdot \hat{\mathbf{u}}_{\perp}\right)\right] + S_{1q}\, \left[\mathcal{E}_{||}\, \left(\hat{\epsilon}_q \cdot \hat{\mathbf{u}}_{||}\right) + \mathcal{E}_{\perp}\, \left(\hat{\epsilon}_q \cdot \hat{\mathbf{u}}_{\perp}\right)\right] \tag{39}$$

By taking the time average of $|E_1|^2$, after some simplification, we obtain,

$$\begin{aligned}\langle E_1 \cdot E_1^* \rangle \;=\;& |S_{1p}|^2 \left[|\mathcal{E}_{||}|^2\, \left|\hat{\epsilon}_p \cdot \hat{\mathbf{u}}_{||}\right|^2 + |\mathcal{E}_{\perp}|^2\, |\hat{\epsilon}_p \cdot \hat{\mathbf{u}}_{\perp}|^2\right] \;+\; |S_{1q}|^2 \left[|\mathcal{E}_{||}|^2\, \left|\hat{\epsilon}_q \cdot \hat{\mathbf{u}}_{||}\right|^2 + |\mathcal{E}_{\perp}|^2\, |\hat{\epsilon}_q \cdot \hat{\mathbf{u}}_{\perp}|^2\right] + \\ &+ 2\, |\mathcal{E}_{||}|^2\, \Re e \left\{ \boldsymbol{S_{1p}\, S_{1q}^*}\, \left(\hat{\boldsymbol{\epsilon}}_p \cdot \hat{\mathbf{u}}_{||}\right)\, \left(\hat{\boldsymbol{\epsilon}}_q \cdot \hat{\mathbf{u}}_{||}\right)^* \right\} \;+\; 2\, |\mathcal{E}_{\perp}|^2\, \Re e \left\{ \boldsymbol{S_{1p}\, S_{1q}^*}\, \left(\hat{\boldsymbol{\epsilon}}_p \cdot \hat{\mathbf{u}}_{\perp}\right)\, \left(\hat{\boldsymbol{\epsilon}}_q \cdot \hat{\mathbf{u}}_{\perp}\right)^* \right\}\end{aligned} \tag{40}$$

[4]By reciprocity, the *transmitting* and *receiving* far field distributions are related by: $S_{ip}(\theta, \phi) = S_{pi}^*(\theta, \phi)$ and $S_{iq}(\theta, \phi) = S_{qi}^*(\theta, \phi)$. Also, notice that $|S_{ip}|^2$ and $|S_{iq}|^2$ are the *receiving* co-polar and cross-polar *far field radiation patterns* of the antenna, respectively.

where we have assumed that, for uncorrelated noise sources, $\langle \mathcal{E}_{\|} \cdot \mathcal{E}_{\perp}^{*} \rangle = \langle \mathcal{E}_{\perp} \cdot \mathcal{E}_{\|}^{*} \rangle = 0$,
We can write this also as,

$$\langle E_1 \cdot E_1^{*} \rangle \;=\; P_{1\,\|}\, |\mathcal{E}_{\|}|^2 \;+\; P_{1\perp}\, |\mathcal{E}_{\perp}|^2 \tag{41}$$

with,

$$P_{i\,\|} \;=\; |S_{ip}|^2 \left|\hat{\epsilon}_p \cdot \hat{\mathbf{u}}_{\|}\right|^2 + |S_{iq}|^2 \left|\hat{\epsilon}_q \cdot \hat{\mathbf{u}}_{\|}\right|^2 + 2\,\Re\mathbf{e}\left\{ \boldsymbol{S_{ip}\, S_{iq}^{*}}\ \left(\hat{\boldsymbol{\epsilon}}_{\boldsymbol{p}} \cdot \hat{\mathbf{u}}_{\|}\right)\ \left(\hat{\boldsymbol{\epsilon}}_{\boldsymbol{q}} \cdot \hat{\mathbf{u}}_{\|}\right)^{*} \right\} \tag{42}$$

$$P_{i\perp} \;=\; |S_{ip}|^2 \left|\hat{\epsilon}_p \cdot \hat{\mathbf{u}}_{\perp}\right|^2 + |S_{iq}|^2 \left|\hat{\epsilon}_q \cdot \hat{\mathbf{u}}_{\perp}\right|^2 + 2\,\Re\mathbf{e}\left\{ \boldsymbol{S_{ip}\, S_{iq}^{*}}\ \left(\hat{\boldsymbol{\epsilon}}_{\boldsymbol{p}} \cdot \hat{\mathbf{u}}_{\perp}\right)\ \left(\hat{\boldsymbol{\epsilon}}_{\boldsymbol{q}} \cdot \hat{\mathbf{u}}_{\perp}\right)^{*} \right\} \tag{43}$$

for port $i = \{1, 2\}$.

4.2 Obtaining $T_{b\,\|}$ and $T_{b\,\perp}$

$T_{b\,\|}$ and $T_{b\,\perp}$ are the contributions to the brightness temperature from scattered component of the sky emission plus the emission from the ground, in its appropriate polarization parts, i.e.,

$$T_{b\,\|} \;=\; T_{\|}^{sky} + T_{\|}^{gnd} \tag{44}$$

$$T_{b\,\perp} \;=\; T_{\perp}^{sky} + T_{\perp}^{gnd} \tag{45}$$

The sky noise scattered of the ground is given by,

$$T_{\|}^{sky}(\theta_1) \;=\; \Gamma_{\|}(\theta_1)\, T_b^{sky}(\theta_1) \qquad T_{\perp}^{sky}(\theta_1) \;=\; \Gamma_{\perp}(\theta_1)\, T_b^{sky}(\theta_1) \tag{46}$$

$$T_{\|}^{gnd}(\theta_1) \;=\; \left[1 - \Gamma_{\|}(\theta_1)\right] T_{gnd} \qquad T_{\perp}^{gnd}(\theta_1) \;=\; \left[1 - \Gamma_{\perp}(\theta_1)\right] T_{gnd} \tag{47}$$

where T_b^{sky} is given by Equation 27 and T_{gnd} is the ground temperature, normally assumed to be 300K.
The *power* reflection coefficients at the interface ground-air, $\Gamma_{\|}$ and $\Gamma_{\perp}$, are given by[Ulaby, 1981],

$$\Gamma_{\|}(\theta_1) \;=\; \left| \frac{\cos\theta_1 - \sqrt{\epsilon_2 - \sin^2\theta_1}}{\cos\theta_1 + \sqrt{\epsilon_2 - \sin^2\theta_1}} \right|^2 \tag{48}$$

$$\Gamma_{\perp}(\theta_1) \;=\; \left| \frac{\epsilon_2\ \cos\theta_1 - \sqrt{\epsilon_2 - \sin^2\theta_1}}{\epsilon_2\ \cos\theta_1 + \sqrt{\epsilon_2 - \sin^2\theta_1}} \right|^2 \tag{49}$$

With ϵ_2 is the relative permitivity of the ground.
Therefore, in terms of equivalent noise temperatures from ground emission and scattering, from the sky, the integrand in Equation 2 becomes,

$$T_b(\nu,\theta,\phi)\, P_n(\nu,\theta,\phi\,|\hat{\mathbf{r}}_o) \;=\; \begin{cases} P_n(\nu,\theta,\phi\,|\hat{\mathbf{r}}_o)\, T_b^{sky}(\nu,\theta) & 0 \le \theta < \pi/2 \\ P_{\|}(\nu,\theta,\phi\,|\hat{\mathbf{r}}_o)\ \left[\left(1 - \Gamma_{\|}(\theta_1)\right)\ T_{gnd} + \Gamma_{\|}(\theta_1)\, T_b^{sky}(\theta_1)\right]\ + & \\ \quad +\ P_{\perp}(\nu,\theta,\phi\,|\hat{\mathbf{r}}_o)\ \left[\left(1 - \Gamma_{\perp}(\theta_1)\right)\ T_{gnd} + \Gamma_{\perp}(\theta_1)\, T_b^{sky}(\theta_1)\right] & \pi/2 \le \theta \le \pi \end{cases} \tag{50}$$

where, $\theta_1 = \pi - \theta$, and $P_{\|}$ and $P_{\perp}$ are given by Equation 43, for each port respectively.

4.3 Reduced Expression

For antenna noise calculations, under certain conditions further simplification can be made: first, we assume unpolarized sources. Second, for dry land, $\epsilon_2 \approx 3.5$, $\Gamma_\perp$ and $\Gamma_\parallel$ are not very different from one another. Third, if the far-side lobes of the co-polar radiation antenna pattern are very low compared with the beam maximum (i.e., approximately -40 dB down) and comparable in value to the cross-polar pattern. Fourth, the antenna is not pointing to the ground...

Then, we could define an average reflection coefficient,

$$\tilde{\Gamma}(\theta_1) = \frac{\Gamma_\parallel(\theta_1) + \Gamma_\perp(\theta_1)}{2} \tag{51}$$

and Equation 50 may be written as:

$$T_b(\nu,\theta,\phi)\,P_n(\nu,\theta,\phi\,|\hat{\mathbf{r}}_o) = \begin{cases} P_n(\nu,\theta,\phi\,|\hat{\mathbf{r}}_o)\,T_b^{sky}(\nu,\theta) & 0 \le \theta < \pi/2 \\ P_n(\nu,\theta,\phi\,|\hat{\mathbf{r}}_o)\,\left[\left(1-\tilde{\Gamma}(\theta_1)\right)\,T_{gnd} + \tilde{\Gamma}(\theta_1)\,T_b^{sky}(\theta_1)\right] & \pi/2 \le \theta \le \pi \end{cases} \tag{52}$$

Equation 52 is an *estimate* to the ground emission and scattering, and in general Equation 50 should be used instead.

References

[Giardino et al. 2002] G.Giardino, A.J.Banday, K.M. Górski, K.Bennett, J.L.Jonas, and J.Tauber, "Towards a model of full-sky Galactic Synchrotron Intensity and Linear Polarization: A re-analysis of the Parkes Data. *Astronomy and Astrophysics.* Vol 387, p. 82-97, 2002.

[Grossman, 1989] E. Grossman, *AT atmospheric transmission software*, Airhead Software, Boulder, CO (1989).

[Han & Westwater, 2000] Yogg Han and Ed. R. Westwater, "Analysis and Improvement of Tipping Calibration for Ground-Based Microwave Radiometers". *IEEE Transactions on Geoscience and Remote Sensing.* Vol 38, No. 3, May 2000.

[Haslam et al., 1982] C.G.T. Haslam, C.J. Salter, H. Stoffel and W.E. Wilson "A 408 MHz all-sky continuum survey.II. The Atlas of Contour Maps" *Astronomy and Astrophysics Supplement Series*, Vol. 47, pp. 1-143, Jan. 1982.

[Janssen, 1993] Michael A. Janssen, Editor "An Introduction to the Passive Microwave Remote Sensing of Atmospheres". *Atmospheric Remote Sensing by Microwave Radiometry* John Wiley & Sons, New York, ch. 1, 1993.

[Lawson et al., 1987] K.D. Lawson, C.J. Mayer, J.L. Osborne and M.L. Parkinson, "Variations in the spectral index of the galactic radio continuum emission in the northern hemisphere". *Mon. Not. Royal Astronomical Society.* Vol 225, p. 307-327, 1987.

[Liebe, 1989] H. J. Liebe, "MPM-An Atmospheric Millimeter-wave Propagation Model" *International Journal of Infrared and Millimeter Waves*, Vol. 10, No. 6, 1989.

[Merzbacher, 1970] E. Merzbacher, *Quantum Mechanics*, John Wiley & Sons, 2nd. Ed. ch. 4, 1970.

[Pardo et al. 2001] J.R. Pardo, J. Cernicharo and E. Serabyn, "Atmospheric Transmission at Microwaves (ATM): An Improved Model for Millimeter/Sub-Millimeter Applications *IEEE Trans. Antennas and Propagation* Vol AP-49, pp. 1683-1694, No. 12 Dec. 2001.

[Pickett et al., 1998] H.M. Pickett, R.L. Poynter, E.A. Cohen, M.L. Delitsky, J.C. Pearson and H.S.P. Müller, "Submillimeter, Millimeter and Microwave Spectral Line Catalog" *J. Quantitative Spectroscopy Radiative Transfer* Vol 60, No.5 pp. 883-890, 1998.

[Rosenkranz, 1993] P. W. Rosenkranz, "Absorption of Microwaves by Atmospheric Gases". *Atmospheric Remote Sensing by Microwave Radiometry* M. A. Janssen, Editor, John Wiley & Sons, New York, 1993.

[Rosenkranz, 1975] P. W. Rosenkranz, "Shape of the 5mm Oxygen Band in the Atmosphere". *IEEE Trans. Antennas and Propagation* Vol AP-23, pp. 498-506, 1975.

[Rothman et al., 1992] L.S. Rothman, R.R. Gamache, R.H. Tipping, C.P. Rinsland, M.A.H. Smith, D.B. Chris, V.D. Malathy, J.-M Flaud, C. Camy-Peyret, A. Perrin, A. Goldman, S.T. Massie, L.R. Brown, and R.A. Toth, "HITRAN dtabase: 1991 and 1992 editions". *J. Quantitative Spectroscopy Radiative Transfer* Vol 48, pp. 469-507, 1992.

[Waters, 1976] J. Waters,"Absorption and Emission by Atmospheric Gases". In *Methods of Experimental Physics*, Vol 12B, M. Meeks, Ed., Academic Press, New York, 1976, pp. 142-176.

[Ulaby, 1981] F.T. Ulaby, R.K. Moore and A.K. Fung, *Microwave Remote Sensing*,Vol I Addison-Wesley Publishing Company, ch. 4-5, 1981.